The orthorhombic to tetragonal phase transition in $Bi_{1.75}Te_{0.25}SrNb_{1.75}Hf_{0.25}O_9$

2004 J. Phys.: Condens. Matter 16 4139

(http://iopscience.iop.org/0953-8984/16/23/028)

INSTITUTE OF PHYSICS PUBLISHING JOURNAL OF PHYSICS: CONDENSED MATTER

J. Phys.: Condens. Matter **16** (2004) 4139–4148 PII: S0953-8984(04)74553-1

The orthorhombic to tetragonal phase transition in $Bi_{1.75}Te_{0.25}SrNb_{1.75}Hf_{0.25}O_9$

R E Alonso[1], A P Ayala[2], A Castro[3], J J Lima Silva[2], A López-García[1] and A R Paschoal[2]

[1] Departamento de Física, Universidad Nacional de La Plata, La Plata, Argentina
[2] Departamento de Física, Universidade Federal do Ceará, Fortaleza, Brazil
[3] Instituto de Ciencia de Materiales de Madrid, CSIC, Madrid, Spain

Received 8 January 2004
Published 28 May 2004
Online at stacks.iop.org/JPhysCM/16/4139
DOI: 10.1088/0953-8984/16/23/028

Abstract

The necessity to produce materials with better performances than those observed in ferroelectric perovskites has generated the creation of new oxides, especially those belonging to the Aurivillius family. In the last few years much attention has been paid to the study of these materials, and this has opened up new fields due to their basic and applied properties. In this contribution a Raman analysis and a hyperfine study by perturbed angular correlations spectroscopy of $Bi_{1.75}Te_{0.25}SrNb_{1.75}Hf_{0.25}O_9$ were carried out to reveal information about the lattice and the electronic structure. By the use of these techniques, it was observed that the ferroelectric to paraelectric phase transition at about 570 K is driven by a soft mode, and the broadening of the dielectric constant as a function of temperature previously observed at T_C is connected to disorder in the Bi/Te–O layer.

1. Introduction

Layered Bi-oxides, $Bi_2A_{n-1}B_nO_{3n+3}$, belonging to the Aurivillius family, have received renewed interest in the last few years owing to their ferroelectric properties, which have superior performance over those of the commonly employed PZT solid solution ceramics used in memory devices [1].

The structure of these materials can be described by the build up of two different blocks of $[Bi_2O_2]^{2+}$ and $[A_{n-1}B_nO_{3n+1}]^{2-}$, stacked in a crystal structure along the *c*-axis [2]. The $[Bi_2O_2]$ slabs exhibit a red-PbO structure type, where Bi^{3+} is generally the unique cation present, although in some cases it is partially substituted by other cations possessing, like Bi^{3+}, a ns^2 lone pair of valence electrons [3–6]. The $[A_{n-1}B_nO_{3n+1}]$ layer has a pseudo-perovskite structure, where the A site is occupied by a voluminous cation showing cuboctahedral coordination, such as Bi^{3+}, Ln^{3+} (Ln = La, Pr, Nd, Sm, ...), Pb^{2+}, Ca^{2+}, Sr^{2+}, Ba^{2+}, etc, and the B site correspond

to a cation with octahedral coordination, like Ti^{4+}, Zr^{4+}, Hf^{4+}, V^{4+}, V^{5+}, Nb^{5+}, Ta^{5+}, W^{6+}, etc. The n value represents the number of BO_6 octahedrons linking the $[Bi_2O_2]$ slabs.

It is well known that in the Aurivillius phases ferroelectricity originates from structural distortions, mainly in the perovskite slabs [7–10]. So, the structural modifications induced by the crystal site selective substitution of cations should be a very good tool to design the ferroelectric properties of these materials [11]. In this way, the solid solution $[Bi_{2-x}Te_xO_2]^{(2+x)+}[SrNb_{2-x}B_xO_7]^{(2+x)-}$ (B = Ti, Zr, Hf; $0 \leqslant x \leqslant 0.5$) was prepared with a compensated doping for both layers in the $SrBi_2Nb_2O_9$ Aurivillius phase (SBN), where the charge balance between layers was modified. Depoling experiments of ceramics with $x = 0$, 0.25 and 0.5 show that the Curie temperature of these materials increases with increasing the averaged electronegativity value of the cations occupying the B site [12], while the tellurium inclusion in the $[Bi_2O_2]$ layer seems to have minor influence on the ferroelectric behaviour of the material.

Hf substitution with $x = 0.25$ and 0.50 has been studied previously by Durán-Martín *et al* [12]. In both materials, the orthorhombic structure was corroborated by x-ray power diffraction studies at room temperature. In that work, DTA, TG and dielectric measurements for samples with $x = 0.25$ suggested that a ferroelectric to paraelectric phase transition occurs at ≈570 K. It was concluded that this phase transition is not first order but diffuse.

Raman scattering (RS) is a powerful technique to investigate structural phase transitions in ferroelectric Aurivillius phases. A review of the most relevant results on this field was recently published by Dobal and Katiyar [13]. As a rule, the ferro–paraelectric phase transition is characterized by a soft mode around 30 cm^{-1}. Decreasing the size of the A cation, the soft mode changes from over-damped to under-damped. On the other hand, the substitution of the B site by heavier cations moves the soft mode toward higher energies.

The determination of the nuclear hyperfine interaction by means of perturbed angular correlation (PAC) spectroscopy can reveal information about the electronic structure of these materials. This technique was successfully used to investigate several ferroelectric compounds [14]. Since probes are placed inside the oxygen octahedrons, PAC spectroscopy can provide valuable information about the charge distribution in these groups, which are responsible for the ferroelectricity in the Aurivillius compounds. Nevertheless, this technique was never used before to study this family of materials.

The aim of this work is to analyse in the Aurivillius phase $Bi_{2-x}Te_xSrNb_{2-x}Hf_xO_9$ with $x = 0.25$, the mechanism of the ferroelectric–paraelectric phase transition from the temperature dependence of the vibrational modes and the hyperfine interaction by means of RS and PAC.

2. Experimental details

A polycrystalline sample of $Bi_{2-x}Te_xSrNb_{2-x}Hf_xO_9$ with $x = 0.25$ was prepared by conventional solid-state reaction of Bi_2O_3 (Cerac, 99.9% pure), TeO_2 (Cerac, 99.99% pure), $SrCO_3$ (Cerac, 99.5% pure), Nb_2O_5 (Fluka, 99.9% pure) and HfO_2 (Fluka, 99.8% pure). All reactants were homogenized by hand in an agate mortar, in stoichiometric proportions (20% molar excess of TeO_2 was added) to obtain 3 g of the compound. The reaction requires cumulative treatments in order to obtain the Aurivillius phase. Thus, the heating sequence was 20 h at 600, 700, 800 and 850 °C. After each successive step, hand homogenization and characterization by x-ray powder diffraction (XRD) at room temperature were carried out. A Bruker D8 Advance diffractometer was employed to record the XRD patterns, with a scan rate of $0.04°(2\theta)$ s^{-1} from 5° to 60° (2θ), using Cu Kα radiation ($\lambda = 1.5418$ Å).

The Raman study of the sample was carried out using the spectral excitation provided by an argon laser, employing the 488 nm line with a power density of ∼1 MW cm^{-2} on the sample surface. This laser power density was found to optimize the signal-to-noise ratio without overheating the sample. The scattered light was analysed with a Jobin Yvon T64000 spectrometer, equipped with a N_2-cooled charge-coupled device detector. The low-temperature measurements were performed using an air products closed-cycle He cryostat that provides temperatures ranging from 7 to 300 K. A Lakeshore controller was used to control the temperature with precision of ∼0.1 K. The high-temperature studies ($T > 300$ K) were performed by using a resistive furnace.

To measure the hyperfine interaction a PAC spectrometer was used. The as-prepared sample was encapsulated in a quartz tube and then irradiated with a flux of about 2×10^{13} thermal neutrons cm^{-2} s^{-1} for 7 h, at approximately 350 K, to produce the probes by means of the nuclear reaction $^{180}Hf + n \rightarrow {}^{181}Hf^* \rightarrow {}^{181}Ta$. The hyperfine interaction was measured with the 0.482 MeV and $5/2^+$ state of ^{181}Ta with nuclear quadrupole moment $Q = 2.5 \times 10^{-24}$ cm^2 [14]. The activity of the irradiated sample was about 300 μCi and the resulting impurity concentration produced by neutron irradiation was in the ppm level. The coincidence spectra were obtained with a two CsF-detectors PAC spectrometer that has a time resolution of about 0.7 ns for the ^{181}Ta energies. To measure these spectra as a function of temperature, the sample was heated up *in situ* in a furnace with thermal stability better than 1 K. These spectra at selected temperatures were obtained after an accumulation time of about one day. From these data the time spectra that display the nuclear spin precession in time were fitted with a damped oscillatory function of the following hyperfine parameters: the quadrupole frequency $\omega_Q = eQV_{ZZ}/[4I(2I-1)]\hbar$, the asymmetry parameter $\eta = [V_{XX} - V_{YY}]/V_{ZZ}$ and the line width $\delta\omega_Q$ that describes lattice imperfections [14]. The quadrupole hyperfine interaction is represented by the three quantities V_{XX}, V_{YY} and V_{ZZ} that are the diagonal elements of the diagonalized electric field gradient (EFG) tensor that depends on the charge distribution around the probe, i.e. the ^{181}Ta nucleus. These components satisfy the Laplace equation $V_{XX} + V_{YY} + V_{ZZ} = 0$ and are related to the charge distribution $\rho(r)$ by

$$V_{ij} = [4\pi\varepsilon_0]^{-1} \int \rho(r)[(3x_i x_j - \delta_{ij} r^2)/r^5]\,\mathrm{d}v \tag{1}$$

where i, j stand for x, y or z.

3. Results and discussion

The increment of a positive charge generated by the substitution of Bi^{3+} for Te^{4+} in the Bi_2O_2 layer has been compensated for by the diminution in the same amount of positive charge in the perovskite-like layer resulting from the substitution of Nb^{5+} for Hf^{4+}. These cations have been selected due to:

(i) Te^{4+} possesses a $5s^2$ lone pair of electrons with a similar stereochemical effect as the $6s^2$ belonging to Bi^{3+}, which permits the retention of the structural framework of the $[Bi_2O_2]$ slabs;
(ii) Hf^{4+} can exhibit the same octahedral coordination as Nb^{5+}, with similar ionic radii [15].

Figure 1 shows the XRD patterns of the single phase of $Bi_{1.75}Te_{0.25}SrNb_{1.75}Hf_{0.25}O_9$ at room temperature which belongs to the classical Aurivillius structural type. The x-ray diffraction profile was analysed by a pattern matching procedure using the Fullprof program [16]. The line shape of the diffraction peaks was generated with pseudo-Voigt functions. The SBN reported structure [17, 18] was used as the starting point of the data

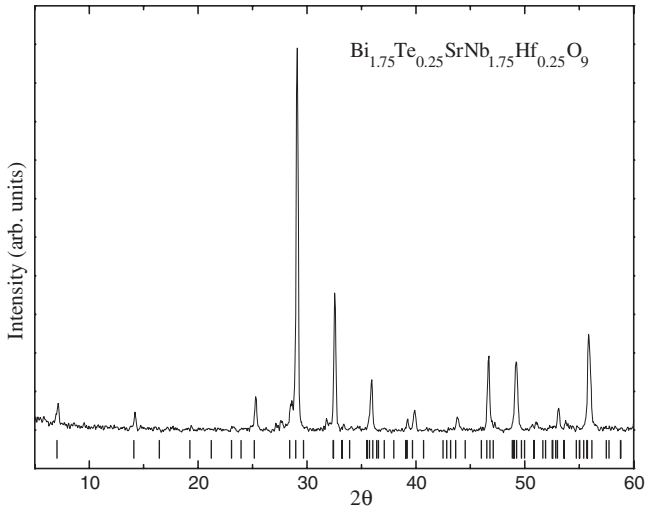

Figure 1. X-ray diffraction pattern of the $Bi_{1.75}Te_{0.25}SrNb_{1.75}Hf_{0.25}O_9$ Aurivillius phase recorded at room temperature.

refinement and this analysis yielded the following parameters: $a = 5.5108$ Å, $b = 5.5146$ Å and $c = 25.0686$ Å. Ferroelectric Aurivillius phases have a tetragonal prototype structure belonging to the $I4/mmm$ (D_{4h}^{17}) space group, and usually transforms into this phase at high temperatures. In the special case of the $n = 2$ family, the factor group analysis yields the following irreducible representation [19]

$$\Gamma = 4A_{1g}(R) + 2B_{1g}(R) + 6E_g(R) + 7A_{2u}(IR) + B_{2u}(IR) + 8E_u(IR). \tag{2}$$

At room temperature several ferroelectric Aurivillius phases exhibit an orthorhombic structure, which average the non-polar $Fmmm$ space group. Polar phases are obtained by small monoclinic or orthorhombic distortions from the $Fmmm$ structure [17]. In the case of $n = 2$ or 4, the ferroelectric phase adopts the orthorhombic $A2_1am$ (C_{2h}^{12}) space group [17, 18]. The irreducible representation of this structure is:

$$\Gamma = 22A_1(R, IR) + 20A_2(R) + 20B_1(R, IR) + 22B_2(R, IR). \tag{3}$$

Figure 2 shows the Raman spectra of $Bi_{1.75}Te_{0.25}SrNb_{1.75}Hf_{0.25}O_9$ recorded at selected temperatures. As can be observed, several wide bands characterize the spectra. Furthermore, no strong changes are detected above the phase transition, which is expected at approximately 575 K [12]. At the critical temperature, the SBN family of compounds transforms directly from the $A2_1am$ phase into the $I4/mmm$ one [20]. Even though the group theory predicts that the number of Raman active modes should be strongly reduced (compare equations (2) and (3)), the occupational disorder characteristic of this family of compounds should activate both infrared modes and phonons outside the centre of Brillouin zone. Thus, it is normal that broken translation symmetry increases the number of Raman active bands. As is usual in the analysis of the Raman spectra of disordered and relaxor ferroelectrics, scattering intensities are written as [21, 22]:

$$I(\nu) = [n(\nu) + 1]I_R(\nu) \tag{4}$$

where $n(\nu)$ is the Bose factor and $I_R(\nu)$ represents the reduced Raman spectrum.

Figure 3 shows the low wavenumber region of the reduced Raman spectra as a function of the temperature. Three Raman bands can be easily identified: the ones around 95 and 60 cm^{-1}

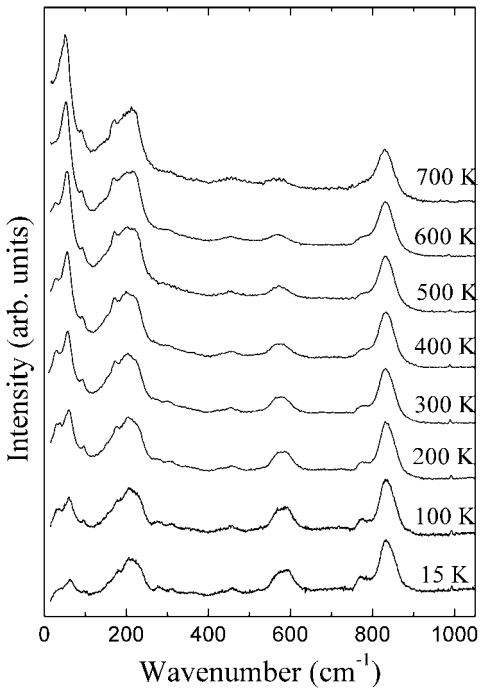

Figure 2. Raman spectra of $Bi_{1.75}Te_{0.25}SrNb_{1.75}Hf_{0.25}O_9$ recorded at selected temperatures.

are observed in the complete temperature range, showing small temperature dependence. On the other hand, the low-lying band, located around 30 cm^{-1} at 15 K, disappear above the critical temperature determined from the dielectric measurements [12]. In figure 4, we plot the temperature dependence of the wavenumber of the low-lying Raman bands. As it can be observed, the low energy band has the typical behaviour of a ferroelectric soft mode. Soft modes in Aurivillius ferroelectrics have been observed in most members of this family. As a rule, the lowest wavenumber band of the Raman spectra of this family can be associated with the soft mode, usually belonging to the A_1 representation [19]. Depending on the cation occupying the A site of the pseudo perovskite unit, the soft mode changes from overdamped (Ba) to underdamped (Sr and Ca). Conversely to the A site substitution, the Bi site substitution by Te does not seem to affect the damping character of the soft mode, since our results show the same underdamped behaviour as that observed in undoped SBN [23]. The increment on the damping of the soft mode due to the A site substitution originates in the larger ionic radius of Ba when compared with Sr [24]. The Bi substitution should induce a similar effect, since these cations are also placed in the octahedral neighbour. However, the Te ionic radius is lower than that of Bi and should induce the opposite behaviour of Ba substitution. It should be interesting to verify if the Bi substitution by a larger cation induces an overdamped behaviour in the soft mode. On the other hand, the B site substitution by a heavier cation hardens the soft mode. That is the case when Ta occupies the Nb site, where the soft mode wavenumber at room temperature decreases from 34 to 29 cm^{-1} [13]. In our case, the partial replacement of Nb by Hf, which has approximately the same atomic weight as Ta, reduces at room temperature the soft mode wavenumber to 30 cm^{-1}, in good agreement with the expected behaviour.

As was pointed out, the occupational disorder, which relaxes the selection rules, together with the small orthorhombic distortion give rise to a similar number of observed Raman

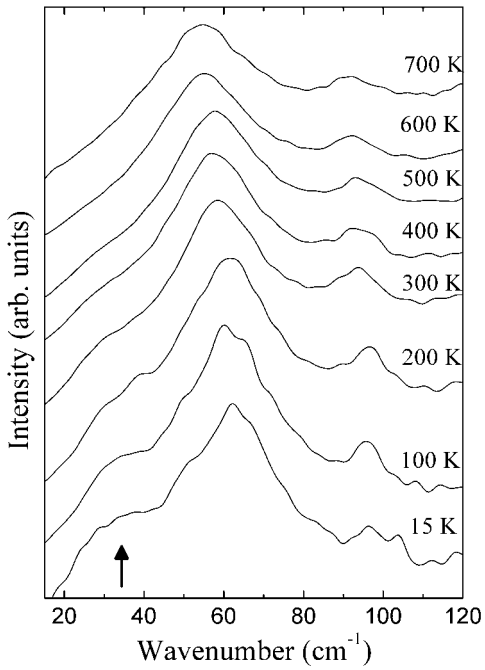

Figure 3. Low wavenumber region of reduced Raman spectra at selected temperatures in $Bi_{1.75}Te_{0.25}SrNb_{1.75}Hf_{0.25}O_9$.

bands in both ferro- and paraelectric phases. However, the nature of the phase transition mechanism can help us to identify additional evidence of the structural transformation. The structural transformation from tetragonal ($I4/mmm$) to orthorhombic ($A2_1am$) is driven by an orthorhombic distortion. The symmetry reduction from $4/mmm$ (D_{4h}) to $mm2$ (C_{2v}) is accompanied by the rotation of the polar axes, which is aligned to the *a* axis in the ferroelectric phase. Thus, the mirror plane (σ_h) perpendicular to the tetragonal axis is retained in the ferroelectric phase and becomes a vertical plane (σ_v), where lie the Sr cations and the O that connects octahedral sites along the *c* axis. According to the normal coordinate analysis presented by Graves *et al* [19], the twofold degenerate E_g modes of the tetragonal phase associated with the movement of the O anions become non-degenerated in the ferroelectric phase ($E_g \rightarrow A_2 + B_2$). Graves *et al* assigned the E_g mode located at approximately 590 cm^{-1} in the high temperature spectra to the vibration of the apical oxygen in the xy-plane in Ti based Aurivillius phases. The symmetry lowering of the apical oxygen was recently observed by powder neutron diffraction, which shows the splitting of the Bi–O_{apical} bond lengths in the ferroelectric phase [20]. As can be observed in figure 5, the Raman band located at ~575 cm^{-1} in the high temperature spectra splits below the critical temperature determined by dielectric measurements, exhibiting the expected behaviour of an E_g mode. Since the Nb doping of Ti based Aurivillius phases softens the ~590 cm^{-1} band [13], it is possible to associate the 575 cm^{-1} band with the E_g mode discussed by Graves *et al* [19]. Notice that the remaining bands do not show any evidence of the phase transition. A similar behaviour should be expected in the other bands belonging to the E_g representation. However, the selection rules relaxation induces a strong overlap of the bands, especially in the low wavenumber region, which avoid the identification of the E_g band splitting.

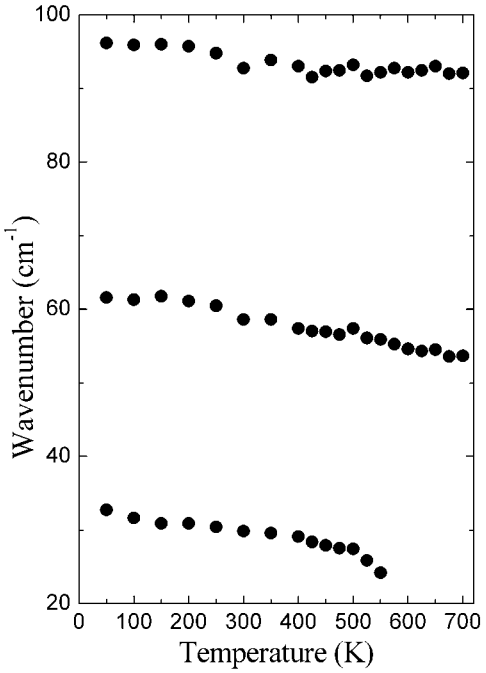

Figure 4. Temperature dependence of the low-lying vibrational bands of $Bi_{1.75}Te_{0.25}SrNb_{1.75}Hf_{0.25}O_9$.

The time spectra obtained with the PAC spectrometer were fitted with a unique electric quadrupole, asymmetric and distributed hyperfine interaction indicating that all probes sit in equivalent positions. Due to the preparation method this position should correspond to probes at the B site. In figure 6 the temperature dependence of the hyperfine parameters is shown.

At room temperature the fitted values are the quadrupole frequency $\omega_Q = 117_1$ Mrad s^{-1}, the asymmetry parameter $\eta = 0.34_2$ and the line width $\delta = 6_1\%$ ($\delta\omega_Q = 6.8_{1.1}$ Mrad s^{-1}). These hyperfine parameters correspond to the orthorhombic structure. In the $SrHfO_3$ perovskite, which also has an orthorhombic lattice at room temperature, it was found that $\omega_Q = 19.8_3$ Mrad s^{-1}, $\eta = 0.47_2$ and $\delta = 24_2\%$ [24]. Comparing the respective values of ω_Q (or the intensity of V_{ZZ}), an increment of a factor $\sim$6 is observed (see below).

The temperature dependence of ω_Q and η indicates that there is a jump between 540 and 590 K in both hyperfine parameters. The quadrupole frequency is almost temperature independent below 540 K. Above 590 K is also constant but at a lower value. The behaviour of η is similar; constant with temperature in both phases except that it is more asymmetric in the tetragonal phase.

Contrary to ferroelectric perovskites in the Aurivillius phases the oxygen octahedrons are surrounded by two different cations (Sr and Bi(Te)), with different atomic radii, thus inducing a strong distortion in the octahedrons. This effect originates the spontaneous ferroelectric polarization along the $\boldsymbol{a}$ axis in the orthorhombic phase [25]. Furthermore, when the central cation is Nb, the Bi_2O_2 layers have a small participation in the spontaneous polarization, which mainly comes from the oxygen octahedron [26]. The strong distortions of the octahedron have direct influence on the hyperfine parameters, giving rise to the high quadrupolar frequency (ω_Q) observed at room temperature compared to that of $SrHfO_3$.

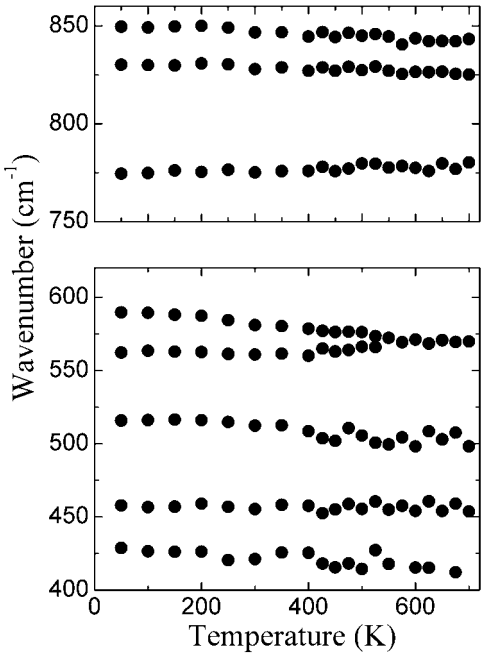

Figure 5. Temperature dependence of the high wavenumber vibrational bands of $Bi_{1.75}Te_{0.25}SrNb_{1.75}Hf_{0.25}O_9$.

Another difference between the perovskites and Aurivillius phases is related to the behaviour of the paraelectric phase. While in the first family the oxygen octahedrons are regular, this group in the Aurivillius phases is still distorted above the critical temperature. The ferro–paraelectric phase transition mechanism in the last compound is produced by ion displacements along the polar axis (**a** axis) that brings these ions into positions where the dipole moments are zero. These effects produce a ∼2% reduction in the quadrupole frequency. Using the point charge model the dipole moment contribution to ω_Q is of the order of $l/(a/2)$, l being the 'dipole length'. Assuming a lattice constant of 5 Å, then $l \approx 0.01$ Å.

In the measured temperature range the line width of the hyperfine interaction δ remains constant with an approximated value of about 5%. This result indicates that passing through the phase transition temperature the disorder at probes does not change at all. This effect was also detected as for example in $Sr_{0.5}Ba_{0.5}HfO_3$. For this compound, the line width is wider ($\delta \approx 20\%$) and also constant with the temperature, even though a second order tetragonal to cubic phase transition takes place at $T_C \sim 700$ K. However, in most perovskites a strong dependence of δ on the temperature is observed. In these cases, the disorder was supposed to be produced by a random distribution of polarized defects, probably oxygen vacancies [27].

From dielectric measurements as a function of the temperature, a reversible structural phase transition represented by a broad line was found [12]. The broadening indicates a diffuse phase transition occurring at about 570 K and probably resulting from occupational disorder. This effect was related to random substitution of Bi and Nb cations by Te and Hf, respectively. Consequently, the line width of the hyperfine interaction measured at B site should also reflect this fact. However, the value measured corresponds to structures with a small amount of disorder as it is found in most oxides, where $\delta \approx 2$–4% [28]. The EFG strongly depends on the distribution of cations and anions and on the electron orbitals that belong to them. The *n*s spherical electronic configuration of Bi(Te) cations cannot contribute

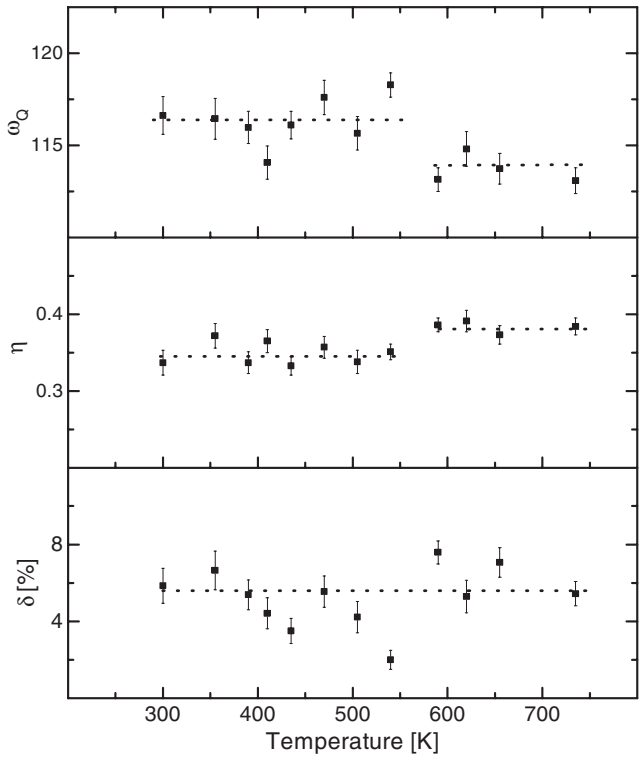

Figure 6. Temperature dependence of the hyperfine parameters of $Bi_{1.75}Te_{0.25}SrNb_{1.75}Hf_{0.25}O_9$. The points are guides to the eye.

to the electric field gradient acting on probes while the np electrons could. Then the line width of $\delta \approx 5\%$ detected by PAC would reflect the occupational disorder in the perovskite layer plus the np electron contribution of the disordered Bi/Te–O layer. It seems that both effects do not have a very important contribution to the line width of the EFG at the probes. Thus, the occupational disorder of the perovskite layer seems to be unimportant and the density of np states in the valence band at the probe neighbour seems to be small. As a consequence, this analysis reveals that it is possible to infer that the broad dielectric peak mainly originates in the Bi/Te–O disordered configurations.

4. Conclusions

The Raman scattering studies of $Bi_{1.75}Te_{0.25}SrNb_{1.75}Hf_{0.25}O_9$ revealed that the diffuse phase transition observed at about 600 K is driven by a low frequency (A_1) soft mode. The phase transition is also evidenced by the splitting of an E_g-like mode at around 575 cm^{-1}, which should be associated with the vibration of the apical oxygen in the xy-plane of the tetragonal phase. From the PAC analyses it is possible to infer that the high quadrupolar frequency is related to the strong distortion of the oxygen octahedrons. The narrow line width of the hyperfine interaction allows us to propose that the origin of the dielectric constant broadening at T_C mainly originates in the disorder of the Bi_2O_2 layers.

Acknowledgments

The present work has been partially supported by MAT2001-0561(MCyT, Spain), 07N/0076/2002(CAM, Spain), CAPES, CNPq and FUNCAP from Brazil, and SECyT, UNLP and CONICET from Argentina.

References

[1] Paz de Araujo C A, Cuchiaro J D, McMillan L D, Scott M C and Scott J F 1995 *Nature* **374** 627
[2] Aurivillius B 1949 *Ark. Kem.* **2** 499
[3] Castro A, Millán P, Martínez-Lope M J and Torrance J B 1993 *Solid State Ion.* **63–65** 897
[4] Millán P, Castro A and Torrance J B 1993 *Mater. Res. Bull.* **28** 117
[5] Ramírez A, Millán P, Castro A and Torrance J B 1994 *Eur. J. Solid State Inorg. Chem.* **31** 173
[6] Millán P, Ramírez A and Castro A 1995 *J. Mater. Sci. Lett.* **14** 1657
[7] Rae A D, Thompson J G, Withers R L and Willis A C 1990 *Acta Crystallogr.* B **46** 474
[8] Rae A D, Thompson J G, Withers R L and Willis A C 1991 *Acta Crystallogr.* B **47** 174
[9] Withers R L, Thompson J G and Rae A D 1991 *J. Solid State Chem.* **94** 404
[10] Rae A D, Thompson J G and Withers R L 1992 *Acta Crystallogr.* B **48** 418
[11] Funakubo H, Watanabe T, Kojima T, Sakai T, Noguchi Y, Miyayama M, Osada M, Kakihana M and Saito K 2003 *J. Cryst. Growth* **248** 180
[12] Durán-Martín P, Jiménez B, Millán P and Castro A 2000 *J. Phys. Chem. Solids* **61** 1423
[13] Dobal P S and Katiyar R S 2002 *J. Raman Spectrosc.* **33** 405 and references therein
[14] Horowitz C, Alonso R E, López-García A, Lamas D G and Caneiro A 2002 *Ferroelectrics* **269** 117
[15] Shannon R D 1976 *Acta Crystallogr.* A **32** 751
[16] Rodríguez-Carvajal J 1990 Fullprof program for Rietveld refinement and pattern matching analysis *15th Congr. Int. Union Crystallography (Tolouse, France, 1990)* www-llb.cea.fr/fullweb/winplotr/winplotr.htm
[17] Withers R L, Thompson J G and Rae A D 1991 *J. Solid State Chem.* **94** 404
[18] Hervoches C H, Snedden A, Riggs R, Kilcoyne S H, Manuel P and Lightfoot P 2002 *J. Solid State Chem.* **164** 280
[19] Graves P R, Hva G, Myhra S and Thompson J G 1995 *J. Solid State Chem.* **114** 112
[20] Snedden A, Hervoches C H and Lightfoot P 2003 *Phys. Rev.* B **67** 92102
[21] Dujovne I, Koo T-Y, Pinczuk A, Cheong S-W and Dennis B S 2002 *Phys. Rev.* B **66** 64110
[22] Kojima S 1998 *J. Phys.: Condens. Matter* **10** L327
[23] Liu J, Zou G, Yang H and Cui Q 1974 *Solid State Commun.* **90** 365
[24] López-García A, de la Presa P and Ayala A P 2001 *J. Solid State Chem.* **159** 1
[25] Blake S M, Falconer M J, McCreedy M and Lightfoot P 1997 *J. Mater. Chem.* **7** 1609
[26] Shimakawa Y, Kubo Y, Tauchi Y, Kamiyama T, Asano H and Izumi F 2000 *Appl. Phys. Lett.* **77** 2749
[27] Alonso R E, Horowitz C, López-García A, Lamas D G and Caneiro A 2001 *Solid State Commun.* **120** 205
[28] Ayala A, Alonso R and López-García A 1994 *Phys. Rev.* B **50** 3547